YOUNAS, M., MARYAM, A., KHAN, M., NAWAZ, A.A., JAFFERY, S.H.I., ANWAR, M.N. and ALI, L. 2019. Parametric analysis of wax printing technique for fabricating microfluidic paper-based analytic devices (µPAD) for milk adulteration analysis. Microfluidics and nanofluidics [online], 23(3), article number 38. Available from: https://doi.org/10.1007/s10404-019-2208-z

Parametric analysis of wax printing technique for fabricating microfluidic paper-based analytic devices (µPAD) for milk adulteration analysis.

YOUNAS, M., MARYAM, A., KHAN, M., NAWAZ, A.A., JAFFERY, S.H.I., ANWAR, M.N. and ALI, L.

2019

This version of the article has been accepted for publication, after peer review (when applicable) and is subject to Springer Nature's AM terms of use, but is not the Version of Record and does not reflect post-acceptance improvements, or any corrections. The Version of Record is available online at: https://doi.org/10.1007/s10404-019-2208-z
Supplementary materials are appended after the main text of this document.

OpenAIR @RGU

This document was downloaded from https://openair.rgu.ac.uk

SEE TERMS OF USE IN BOX ABOVE

DISTRIBUTED UNDER LICENCE

Parametric Analysis of Wax Printing Technique for Fabricating Microfluidic Paper-Based Analytic Devices (µPAD) for milk adulteration analysis

Muhammad Younas[a †], Ammara Maryam[a], Mushtaq Khan[a], Ahmad Ahsan Nawaz[a,b] , Syed Husian Imran Jaffery[a,c] , Muhammad Nabeel Anwar[a], Liaqat Ali[a]

[a] *School of Mechanical and Manufacturing Engineering, National University of Science and Technology, Islamabad, 44000, Pakistan.*

[b] *Biotechnologisches Zentrum, Technische Universität Dresden, Tatzberg 47/49, 01307 Dresden, Germany*

[c] *School of Mechanical and Manufacturing Engineering, University of New South Wales, Sydney NSW 2052, Australia*

†Corresponding author:

Muhammad Younas

Current Address: School of Mechanical and Manufacturing Engineering (SMME), National University of Science and Technology (NUST), Sector H-12, Islamabad 44000, Pakistan

Email Address: muhammadyounas.phd@smme.nust.edu.pk

Ph: +92 (0) 312 9594464

This research received no specific grant from any funding agency in the public, commercial, or not-for-profit sectors

Parametric Analysis of Wax Printing Technique for Fabricating Microfluidic Paper-Based Analytic Devices (µPAD) for Milk Adulteration Analysis

Abstract

Accurate prediction of hydrophobic-hydrophilic channel barriers is essential in fabrication of paper based microfluidic devices. This research presents a detailed parametric analysis of wax printing technique for fabricating µPADs. Utilizing commonly used Grade 1 filter paper, experimental results show that the wax spreading in the paper porous structure depends on the initially deposited wax line thickness, a threshold melting temperature and melting time. Initial width of the printed line has a linear relationship with the final width of the barrier; however, a less pronounced effect of temperature was observed. Based on the spreading behavior of the molten wax at different parameters, a generalized regression model has been developed and validated experimentally. The developed model accurately predicts wax spreading in Whatman filter paper paper: a non-uniform distribution of pores and fibers. Finally, tests were carried out for calorimetric detection of commonly used adulterants present in milk samples.

Keywords
Paper based, microfluidics, fabrication, wax printing, analytical devices, milk adulterants

Symbols

L	Average wax spreading from the edges of printed line	F_{HC}	Final Hydrophilic channel width
I	Width of printed line	I_{HC}	Initial Hydrophilic channel width
T	Melting temperature	D	Pore size
t	Melting time	Γ	Surface tension
η	Viscosity	μm	Micrometer
ESI	Electronic supplementary Information		

1 Introduction

Paper based microfluidics is a broad group of analytical devices (µPADs) that makes use of complex biochemical samples containing macromolecules, proteins, nucleic acids, toxins, cells or pathogens for analysis. These devices have significant potential for use in diverse application areas including point of care diagnostics, environmental regulations and food quality monitoring [1]. In recent years, µPADs have emerged as a research area of interest for detection and diagnosis in many applications because of their simple fabrication, low cost, flexibility, user friendly functioning [2-4]. Properties like good biological compatibility, strong capillarity, ease of fabrication, disposability and easy availability of µPADs make them unique, when compared to conventional devices made of polymer and/or glass substrates [5-7].

Various techniques used for patterning paper includes wax printing [8, 9] wax screen printing [10, 11], paper cutting[12], inkjet printing[13-15] photolithography[3], wax dipping [16], analogue plotting[17], etching[18], plasma treatment [19, 20] and laser treatment [21]. The hydrophilic-hydrophobic microchannel contrast of the paper network makes these devices suitable for handling small volumes of fluid for quantitative analysis of many potential applications in healthcare, medicine, quality control and environmental monitoring.

Carrilho *et al.* [8] in 2009 introduced an inexpensive, fast and efficient process of wax printing for patterning paper-based microfluidic devices in less than 5 minutes. A simple equation based on well-developed Washburn's equation was presented to predict the wax spreading (L) and width of the hydrophobic barriers (W_B) for initially printed line width (W_P).

$$W_B = W_P + 2L \quad \textbf{(1)}$$

$$L = (\gamma D t / 4\eta)^{1/2} \quad \textbf{(2)}$$

This model proposes that the wax spreading is proportional to square root of time. Dungchai *et al.* [10] applied wax screen printing method and produced paper microfluidic devices on Grade 1 filter paper. The final width of the hydrophobic barriers was related to the wax spreading in the paper (predicted from Washburn equation) indicated by a linear equation. Renault *et al*. [22] studied wax transport in Whatman Grade 1 filter paper and 3MM chromatography paper, and the resulting final width of the barrier was also predicted by Washburn's equation. Zhong *et al.* [23] investigated different paper material and wax types for fabricating optimal μPAD device and applied Washburn's equation to study the mechanics of fluid flow in the hydrophilic channel. Lu *et. al.[24]* used three different methods to pattern paper using wax and performed bioassays. The resulting width of the final hydrophobic barrier was estimated from the difference between original printed line and the final spread line after heating step. One of the biggest challenges of the microfluidic research today is the precise control of reagents within the µPAD device which require an accurate patterning method. To develop an accurate paper-based device by a wax printing technique, an effective model is required to accurately predict the spreading of wax in the paper. This will enable prediction of the channel/ barrier final dimensions for guiding the fluidic flow within the paper network. Many researchers have proposed Washburn equation for this purpose; however, one common limitation of the Washburn's model is the approximation of paper fiber structure as a bundle of capillaries assuming the representative pore size of the paper as the capillary radius (D). Whereas, on the micro scale, the paper has a highly complex fibrous structure with interfiber pores and intra-fiber pores exhibiting a large pore size distribution within the paper surface [25]. Hence, assuming the representative pore size of the paper as capillary radius results in inaccuracy in predicting the wax spreading in the paper. In addition, the Washburn's equation can only be applied to capillary flow under constant driving pressure (infinite reservoir) , during the capillary flow process [26]. However, wax spreading encounters significant pressure change as the wax spreads in the pores of the paper with a limited volume of wax deposited on its surface during the printing process.

This research focuses on wax printing method due to its simplilicity i.e. using solid wax-based ink printer and a hot plate. The presented method eliminates the use of the clean room, UV lamps, organic solvent or other sophisticated instrumentation used in other methods [9]. In this work we performed a systematic series of experiments to observe the spreading of molten wax in the paper at varying temperature, initital deposited wax and different time. A regression model was developed which relates these parameters to the final achieved hydrophobic barrier width (channel dimensions). This study also employed μPAD-based analytical device for the detection of commonly used adulterants present in milk samples. Tests were carried out for neutralizers, urea and detergents in milk samples. In order to check the functionality of device, adulterants were intentionally added to the sample. Specific reagents were used for particular reactions. These particular tests and the composition of reagents were based on the specific chemical reactions [27].

2 Materials and methods

2.1 Materials

The Whatman Grade 1 filter paper available in sheets of 46 cm × 570 cm were chosen as substrate material for fabricating µPAD. The desired patterns were first drawn using AutoCAD where the initially printed line thickness was varied from 100 µm to 900 µm. These patterns were then printed using Xerox ColorQube 8580 Printer. The thickness of the initially printed line patterns for each set were checked in the microscope before keeping on the hot plate. The reproducibility of the device is highly dependent on the initial printed line width and temperature applied for wax spreading. These printers utilize solid wax based ink composed of hydrocarbons

for printing [28]. To provide a uniformly heated surface, we used an analogue hot plate and a constant temperature of the plate was maintained using IR thermometer. The thickness of lines before and after spreading was measured using an optical microscope. Figure 1 shows schematics of the printing of µPAD.

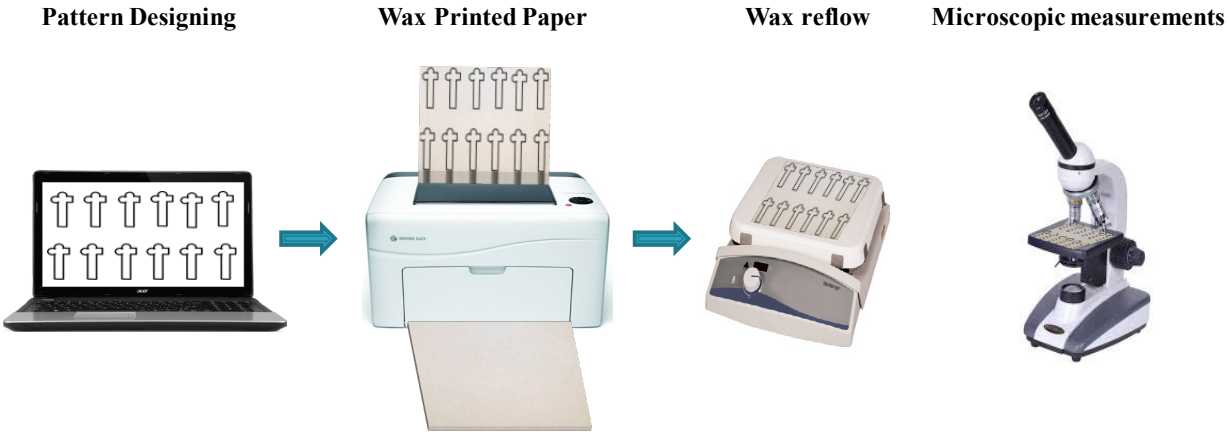

Fig. 1 Overview of wax printing technique for fabricating paper microfluidic device

2.2 Design of experiments

A series of lines of different widths were printed on filter paper, and the resulting final width of the lines was investigated at four different temperatures. Table 1 shows the range of initial printed width, time and temperature for experimentation. The wax spreading for all temperature sets were measured after five seconds interval until complete spreading of the initially printed wax on paper.

Table. 1 Experimental details and parameters

Sr. #	Parameters	Range/Value
1	Initial printed width	100 µm, 200 µm, 300 µm, 400 µm, 500 µm, 600 µm, 700 µm, 800 µm, 900 µm.
2	Time	Reading after every 5 seconds till stability.
3	Temperature	90 °C , 110 °C, 130 °C, 150 °C.

2.3 Measurement of wax spreading in paper

The printed lines, after placing on hot plate, were studied after five seconds interval to observe the change in the width of the line until complete spreading was achieved. The printed lines were studied for the time required for complete melting at different temperatures. Figure 2 shows measurement on a 900 µm printed wax line before and after spreading (at 90ºC). Three readings were taken for each line and the results were averaged.

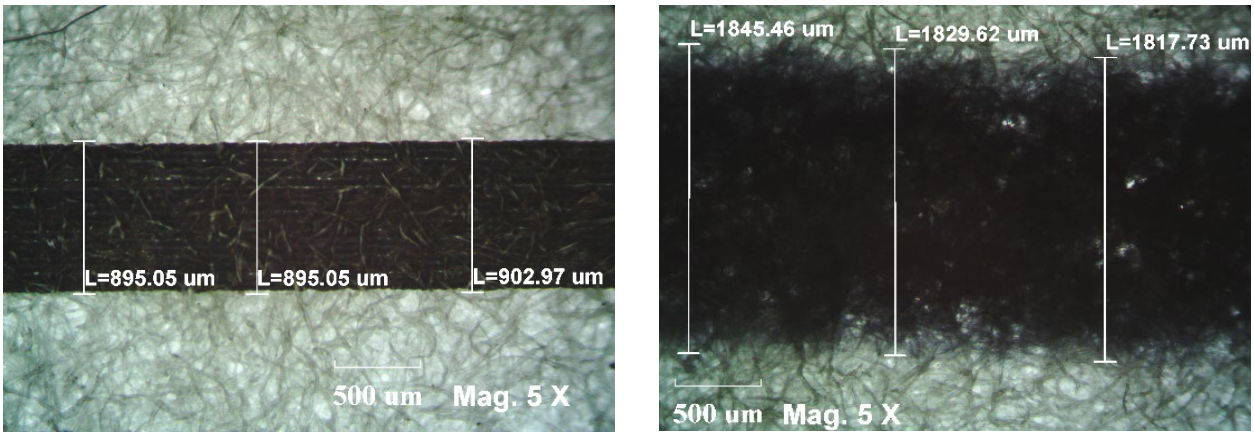

(a) **(b)**

Fig. 2 Optical microscope image of 900µm initial wax line (a) before spreading, (b) after complete spreading at 90ºC

3 Results and discussions

3.1 Experimental conditions study

3.1.1 The effect of temperature on the melting time

A series of lines printed on paper ranging from 100 µm to 900 µm were studied for the optimal time required to complete the spreading of wax in the paper. The maximum time needed for spreading of wax in the paper was recorded at four different temperatures for these printed lines. Spreading time for lines of width 100 µm, 300 µm, 600 µm and 900 µm at four temperatures (90 °C, 110 °C, 130 °C and 150 °C) is shown in ESI Figure 1 (a-d). It was observed that there is dominant effect of melting temperature on the total time required for complete spreading such that at high temperature the wax spreads quickly as compared to lower temperatures. Finally, the total fabrication time for devices at temperatures 90 °C, 110 °C, 130 °C and 150 °C resulted in 240 secs, 120 secs, 95 secs and 70 secs respectively. Figure 3 shows that the wax spreading time within the paper reduces as the temperature is increased from 90 °C to 150 °C.

Tables presents optical microscope images of the spreading of wax printed lines (100, 300 and 900µm) at 90 ºC and 150 ºC and at different time intervals. At higher temperature of the hot plate, the wax spreading within the paper was quick compared to the one at lower temperatures. (ESI Table. 1 and 2)

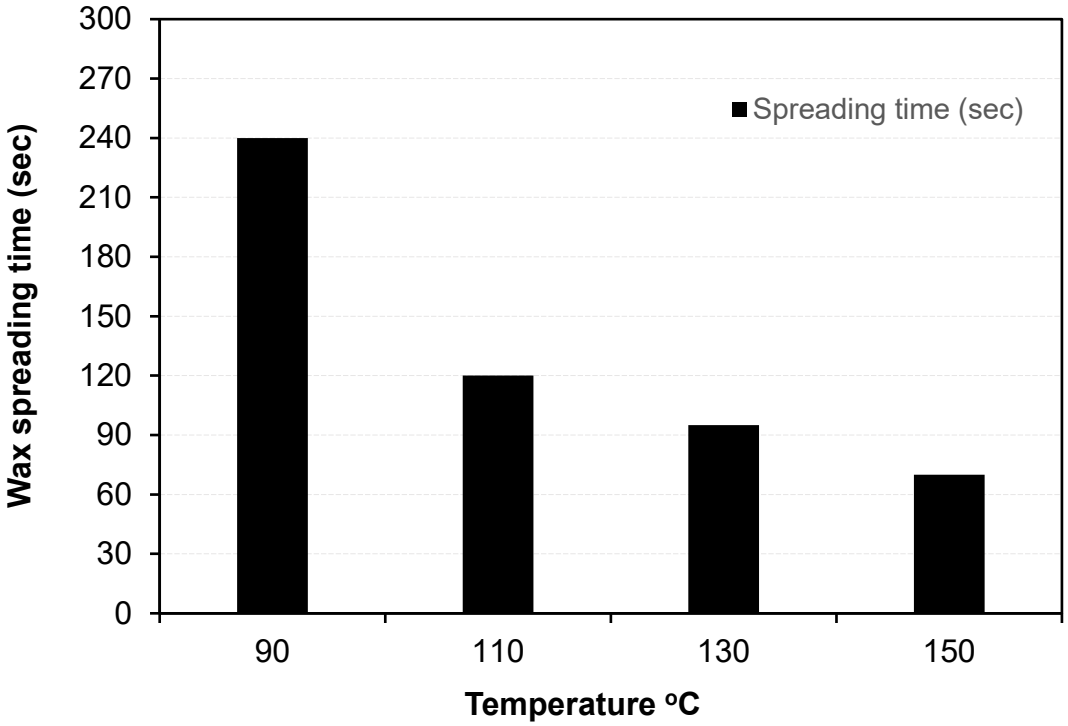

Fig. 3 Effect of temperature on spreading time at four different temperatures

3.1.2 Effect of temperature on the spreading of wax in paper

Figure 4 shows the change in final width of the line at four different temperatures for printed lines 100 µm, 300 µm, 600 µm and 900 µm at four temperatures (90 °C, 110 °C, 130 °C and 150 °C). The results shows that the wax spreads very rapidly in the start of the spreading process as the change from solid phase to liquid phase occurs (first 15 seconds of melting) then it keeps on spreading linearly until all the deposited wax fill the capillaries in the paper (ESI - Figure 2 (a-d)). The increase in the width of the barriers at higher temperature can be explained by taking into account the change in viscosity of wax as the temperature changes, as shown in Figure 5. At higher temperatures (above 100ºC), viscosity of the molten wax is low and makes it flow easily within the capillaries as compared to lower temperatures (90ºC). It can also be observed that for temperature above 100C, there is very less change in the viscosity of the wax, which results in minimal change in the final line width at these temperatures.

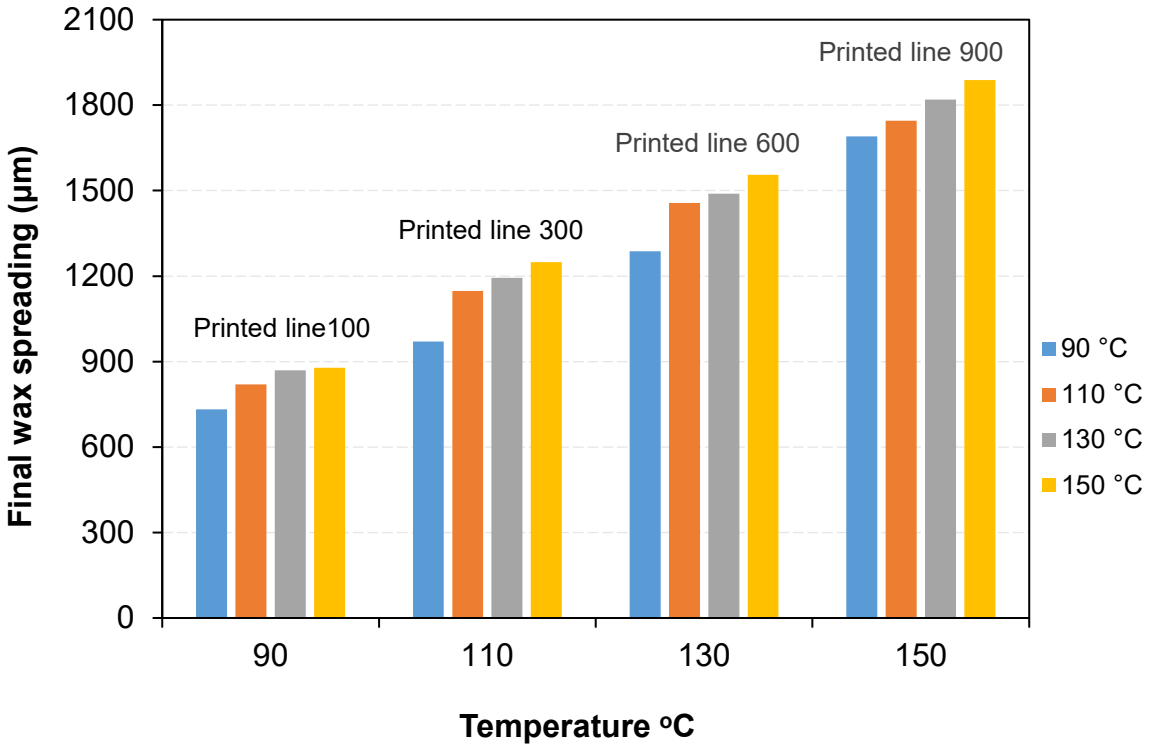

Fig. 4 Effect of temperature on the final width of the printed line

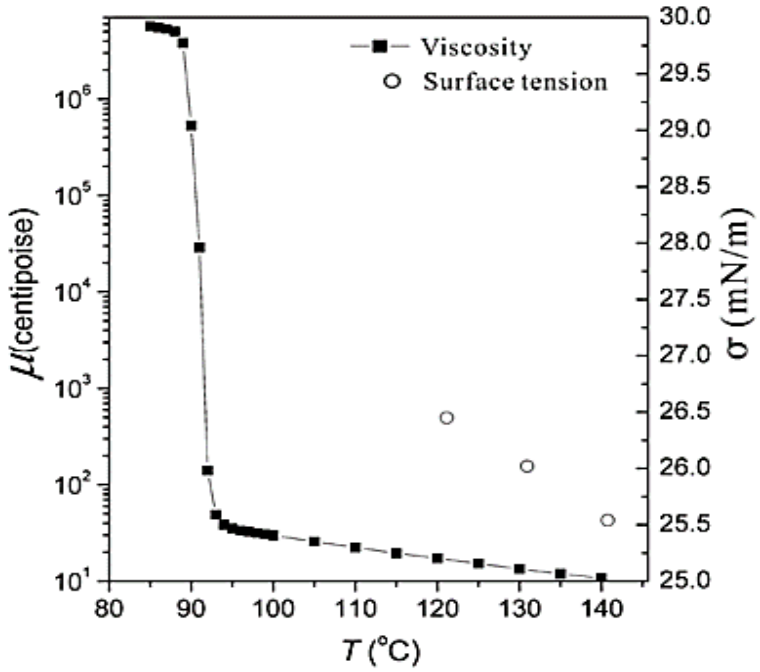

Fig. 5 Viscosity and surface tension of solid ink with varying temperature [29]

3.1.3 Effect of initially printed line width on the final wax spreading

Different initial width lines 100µm to 900 µm were printed on filter paper and studied for its effect on the final width of the hydrophobic barrier at four different temperatures 90 ºC to 150 ºC (Table 1). Initial width of the printed line (Figure 6) has a significant effect on the final width of the barrier; however, varying temperature (beyond 90 ºC) has almost negligible effect. Lines with greater initial thicknesses have a substantial amount of deposited wax, which aids the spreading thus achieving larger final width. The results obtained shows a linear relationship between the initial printed width and final width of the barrier.

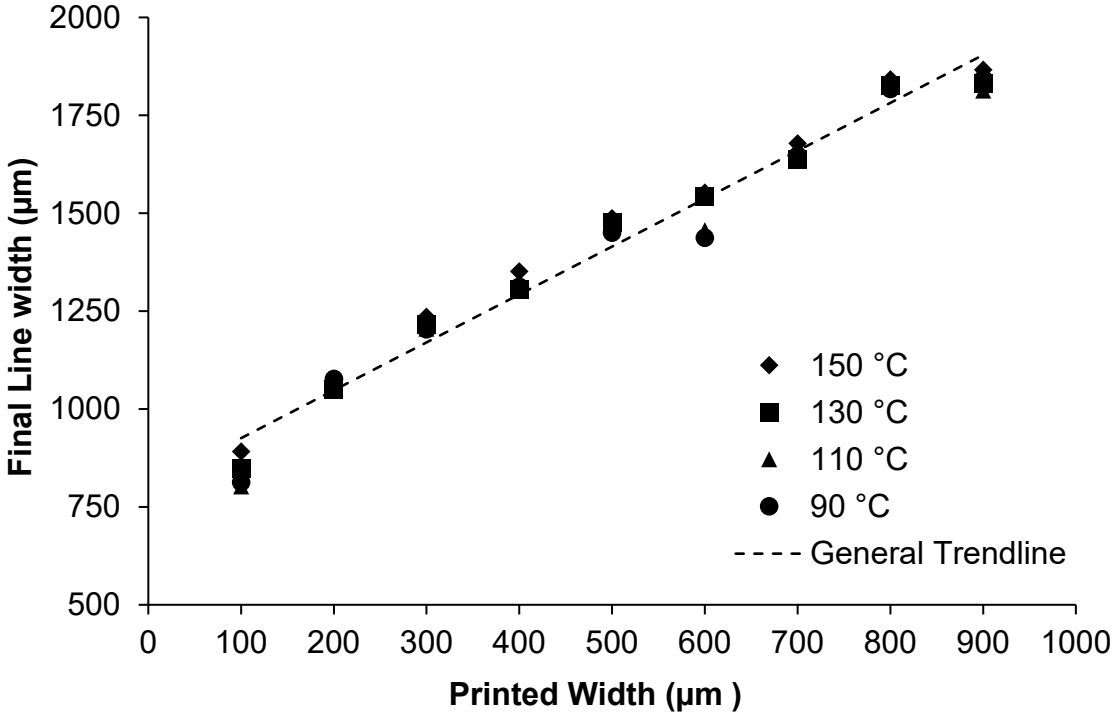

Fig. 6 Width of the wax hydrophobic barrier (line) at temperatures 90ºC, 110ºC, 130ºC and 150ºC after complete spreading

According to the Washburn equation [20], the paper fiber structure is considered as a bundle of capillaries formed by an alignment of pores. However, selecting a representative pore size of the paper as the capillary radius is not a true representation of the pore structure of the paper. Figure 7 shows SEM images of the filter paper with large pore size distribution. A key observation from the SEM micrograph is that the microstructure of paper cannot be accurately approximated as a bundle of cylindrical capillaries, especially considering the practical challenge of measurements of capillary radius from the paper. Also, the Washburn equation applies only to constant pressure capillary flow for unlimited fluid reservoir, whereas, in wax printing, a limited amount is deposited on the paper. The wetting behavior of pores in the paper (Figure 8) also confirms the difference between assumptions of Washburn model for spreading of fluid and actual spreading of wax in the filter paper, where after complete spreading of wax, there is no wax reservoir left on the surface of the paper.

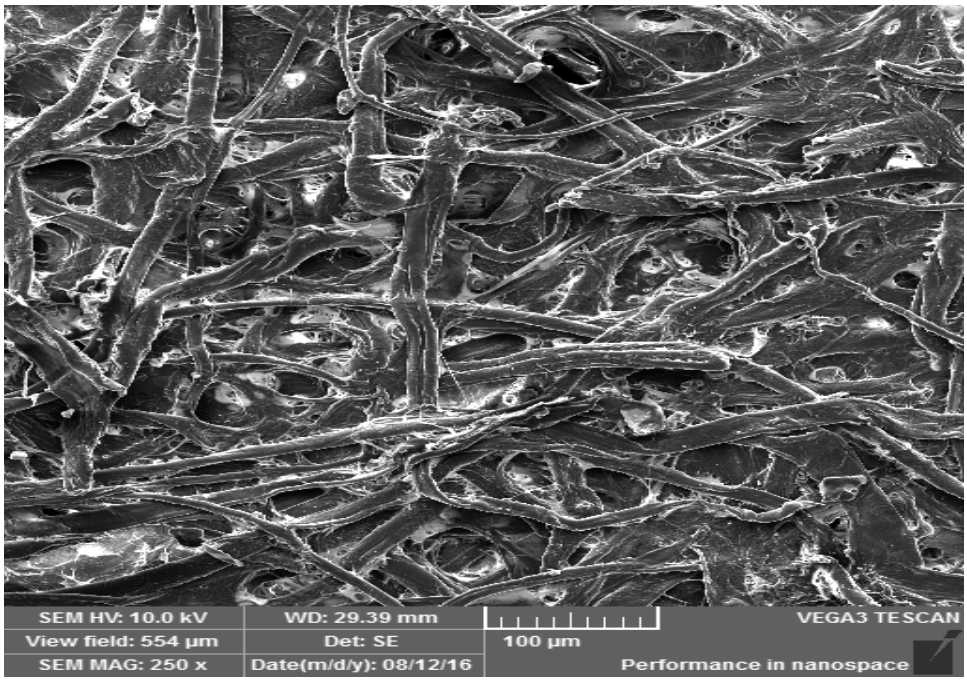

Fig. 7 SEM image of the filter paper showing pores and fiber arrangement

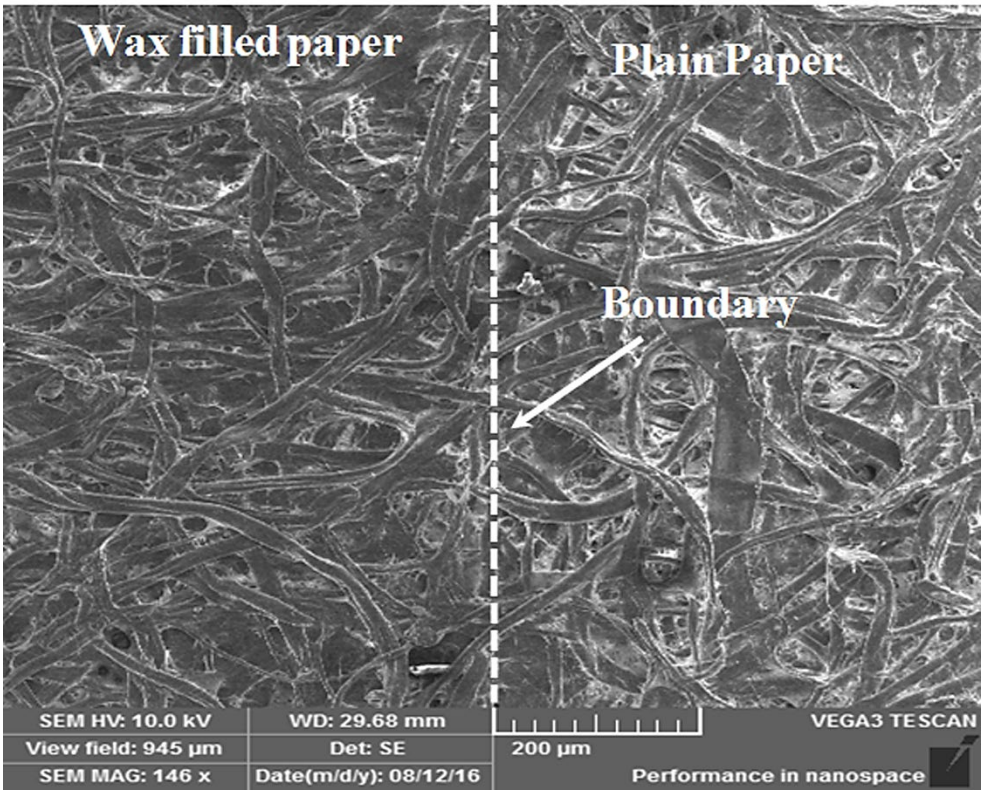

Fig. 8 SEM image of the barrier boundary showing connected pores filled with wax (left side) and plain paper (right side)

3.2 Regression model for spreading of wax in paper

Three important process parameters that were focused during the experimentation were the effect of initially printed width on the final barrier width, the temperature at which the process is carried out and the time for which paper was placed on the hot plate. It is evident from the above results that the wax spreading depends on three important parameters that must be addressed. The results obtained from the experiment were compiled and the data processed in Minitab® Statistical Software using a linear regression to develop an effective model. The resultant model is a function of time (t), temperature (T) and initially printed width (I). The model predicts an accurate response (Y) for the independent variables i.e. t, T and I with an average error of 4% (maximum error of 8 %). The proposed model equation is:

$$\boldsymbol{Y\,(I,t,T) = \mathbf{Exp}\,\{A\ +\ B\ \mathbf{ln}\,(I) +\ C\ \mathbf{ln}\,(t) +\ D\ \mathbf{ln}\,(T)\}} \qquad \textbf{(3)}$$

Where:

A = 3.8111, I = Initial printed line (μm)

B = 0.38644, t = Time (sec)

C = 0.09344 and T = Temperature (ºC)

D = 0.1317.

The above model gives the final width of the hydrophobic barrier for the input values of initially printed line (I), melting time (t) and melting temperature (T).

3.2.1 Width of the hydrophilic channel

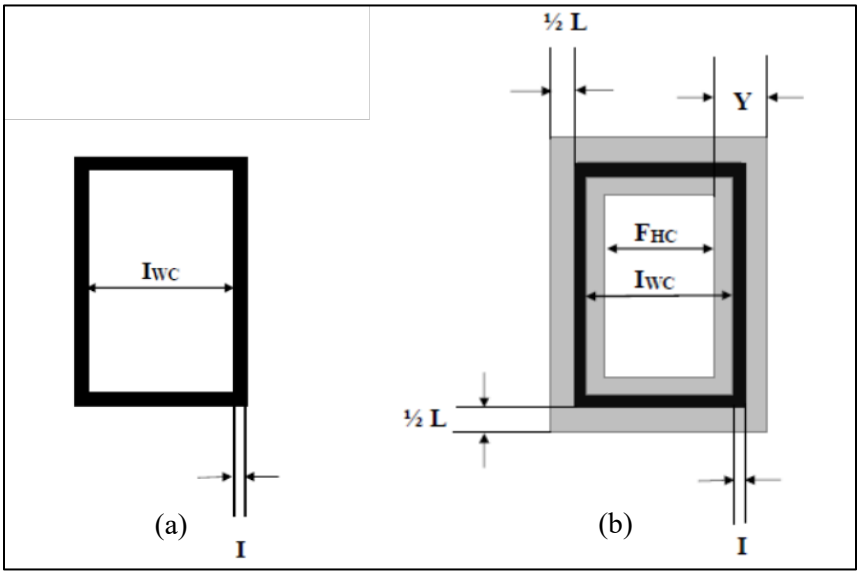

Fig. 9 Schematic representation of the hydrophobic and hydrophilic channels (a) printed channel before spreading and (b) spreading of the wax printed channel after melting

The width of the hydrophilic channel depends on the width of the initially printed line and hence the hydrophobic barrier resulted from the wax spreading. Different channels were fabricated to study the relationship between the width of the hydrophilic channel and the width of initially printed lines. The microscopic analysis was done by measurement

of images of the devices fabricated. The Final width of the hydrophilic channel (F_{HC}) after fabrication is obtained from equation 4 and 5, where I_{WC} is the initial width of the channel before heating step, and L is the final spreading of the printed wax line as shown in Figure 9.

$$F_{HC} = I_{WC} - L \quad (4)$$

And

$$L = Y - I \quad (5)$$

3.2.2 Validation of the regression model

The suggested regression model was validated for additional printed lines of width 150 µm, 350 µm, and 850 µm at temperatures 120 ºC and 140 ºC experimentally and was studied for the complete melting time. A maximum 8 % error was observed in experimental and predicted data from the model. The experimental and predicted data plotted in Figure 10 Shows that the model can best predict the final width of the hydrophobic barrier, by setting all the parameters in the equation. (3). Furthermore, equation. (4 & 5) can be used to define the width of final achieved hydrophilic channel for producing an accurate microfluidic device in the paper.

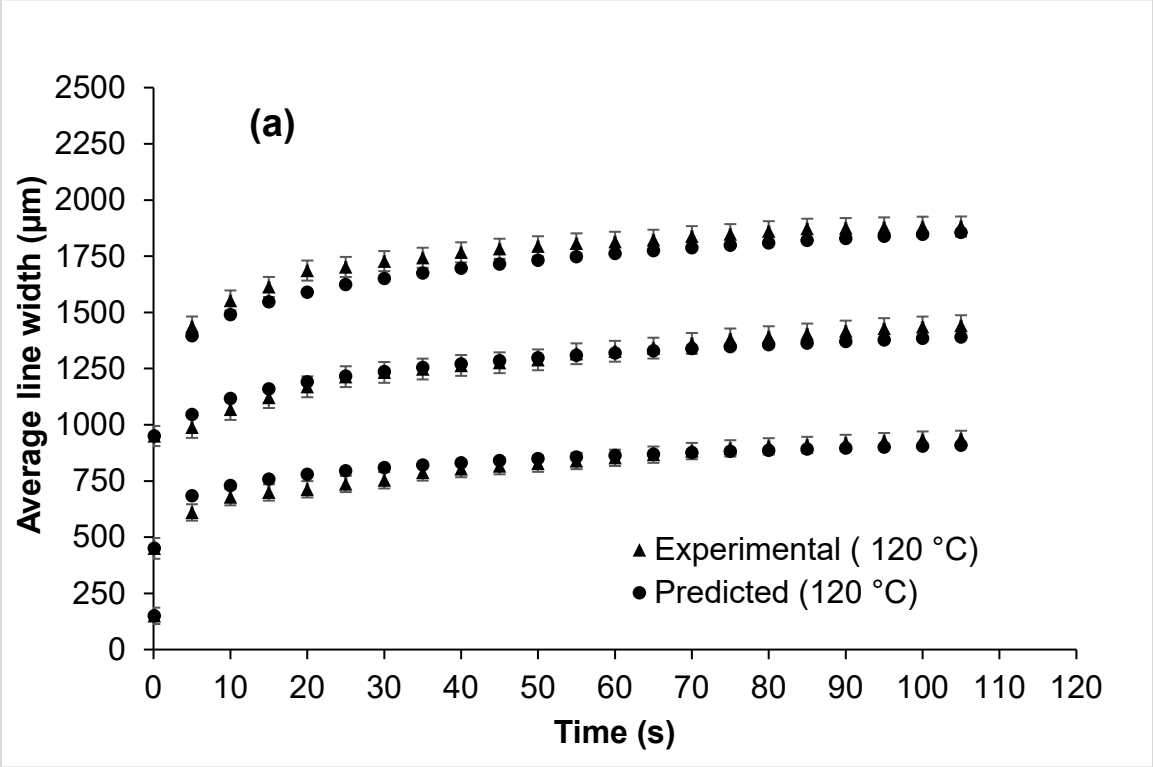

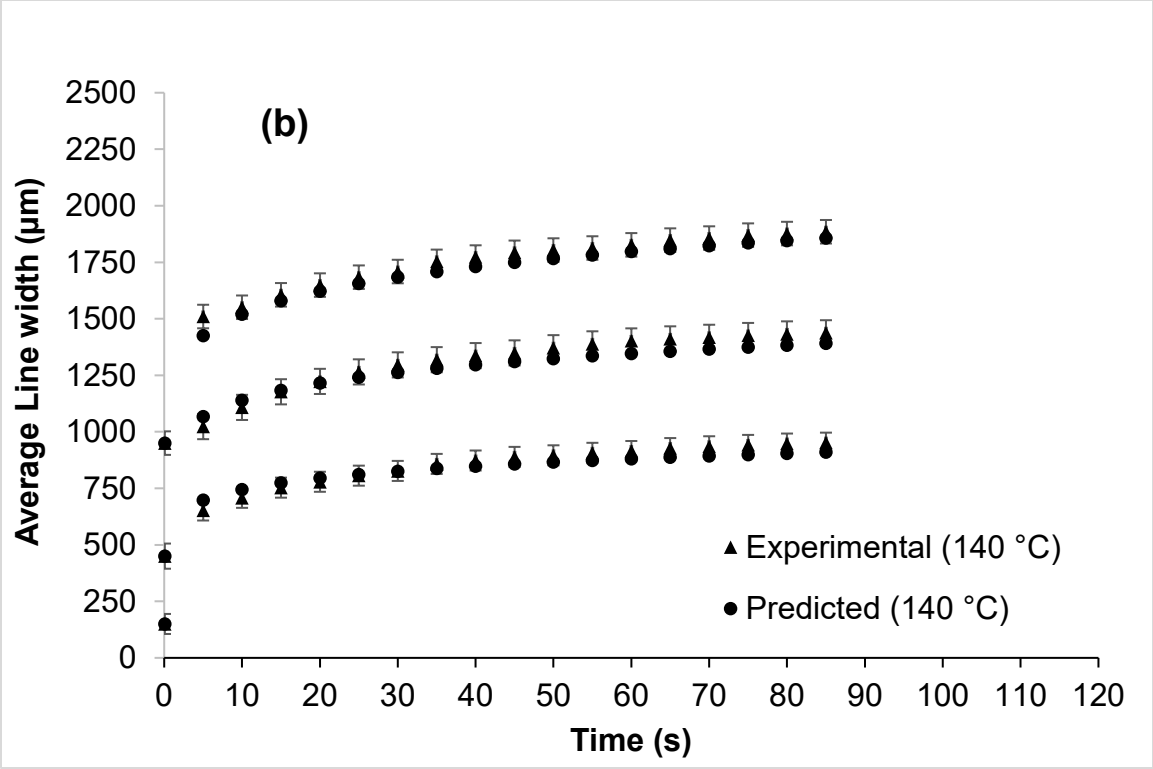

Fig. 10 Graphs showing experimental and predicted trend lines (a) at temperature 120 ºC and (b) at temperature 140 °C. The error bar shows standard deviation final width of three repetitions.

The variations in the trend lines for both the experimental and predicted values can be explained by the complexity of the porous paper involved, the temperature and initial line thickness effect.

The above-developed model is also helpful in predicting the dimension of the wax barrier and channel in applications where high-density features are preferred. The final spreading of the wax line predicted in equation (3) helps the user to change the initial design for maintaining the minimum gap required between the adjacent features to avoid overlap of the final barriers after spreading.

The minimum printed line that produced a functional µPAD had initial printed width of 300 µm resulting an average final line width of 1200 µm. Although, printer can print minimum line width as small as 50 µm but the complex nature of the paper material and the spreading phenomenon limits the minimum functional feature size that can obtained. Series of circle printed with width ranging from 200 µm to 900 µm to check the minimum size of the printed line that result in a functional microfluidic device. Line width less than 300 µm resulted in leakage of the fluid (dye colorant) shown in Figure 11.

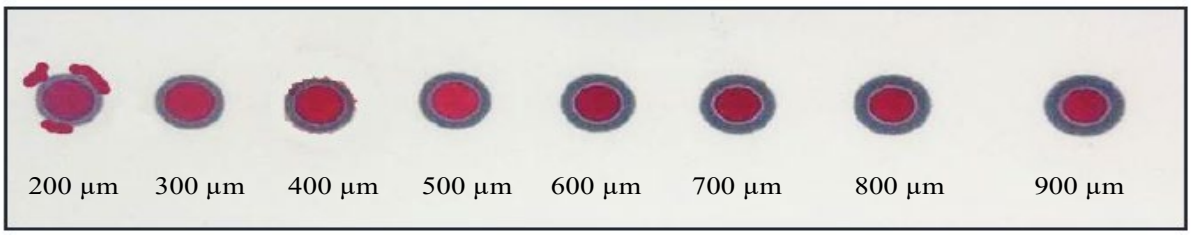

Fig. 11 Sequential increase in line width (200 µm to 900 µm). 300 µm is the the smallest printed line width resulting in a functional µPAD

3.3 Preparation of the device for milk adulteration analysis

Printed-paper was placed on a hot plate set at 150 °C for two to three minutes. This allows the wax to penetrate well throughout the depth of paper. Optimal results were achieved by flipping the paper five to six times over hot plate. The device fabricated for milk adulteration used the best parameters (Temperature 150 ^{0}C and initial printed line 900 µm) that results in a functional µPAD. Equation 3, 4 and 5 were used to predict the width of the hydrophilic channel and wax spreading in the paper. The device comprised of a straight central channel that was divided into three independent test zones. Unique reagents were deposited at all test zones and then dried before the device was ready to use. The volume of the reagents was in the range 0.5-1 μL, depending on the size of each test zone. Sample was applied using micropipette (0-20 μL*)* at the starting point of the central channel. The volume of the sample was 10 μL, flowed by the device into three independent test zones through capillarity. Deposited reagents reacted with sample based on specific chemical reactions. The results were based on easily distinguishable visual colors. After drying completely, the device was ready to use. Solutions for detection of neutralizers (carbonates/bicarbonates), urea and detergents are shown in Table 4.

Table. 4 Reagents for Adulterants

Adulterants	**Reagents**
Detergent	Bromocresol purple solution (0.5%, w/v)
Urea	DMAB Reagent (1.6%, w/v)
Carbonates/Bicarbonates	Rosolic Acid Solution (0.1%, w/v)

3.3.1 Colorimetric tests

Different milk samples of cow and buffalo milk were arbitrarily collected from various areas of Islamabad and Rawalpindi and analyzed for adulteration of neutralizers, urea and detergents. Tests were performed and visual colors (Figure 12) were observed when milk sample reacted with the different reagents in test zones. Tests were carried out for neutralizers, urea and detergents in milk samples. In order to check the functionality of device, adulterants were intentionally added to the sample. This served the purpose for control.

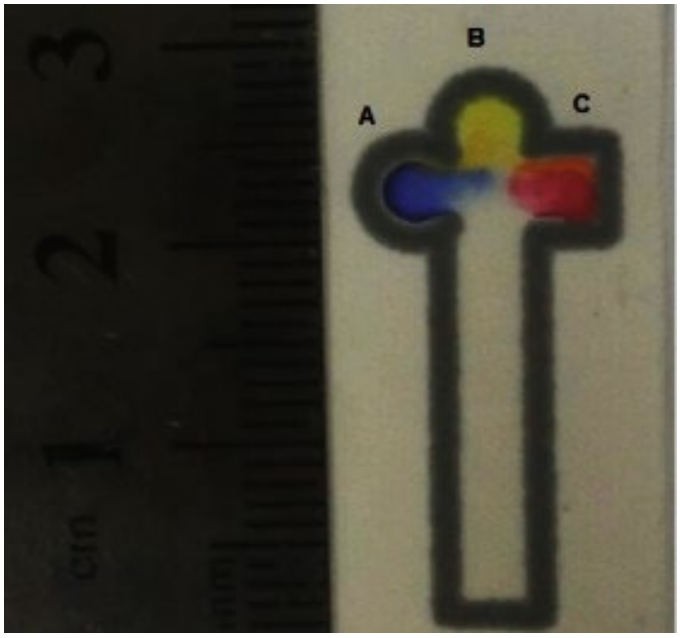

Fig. 12 Wax-printed μPAD for detecting milk adulterants with reagents deposited. Expected visual colors are shown for intentionally adulterated known sample A) Detergent B) Urea C) Carbonates/bicarbonates

Expected colors for the presence or absence of adulterants (detergent, urea, carbonates/bicarbonates) are shown in Table. 5 [27].

Table. 5 Expected colors for the presence or absence of adulterants

Tests	Adulterant/Analyte	Positive/Adulterated	Negative/Pure
A	Detergent	Purple Prominent color	Fade Violet color
B.	Urea	Distinct Yellow color	Faint Yellow color
C.	Carbonates/Bicarbonates	Rose red/Prominent Pink color	Light Brownish color

The results of different milk samples analyzed for various adulterants (detergent, urea, carbonates/bicarbonates) are indicated in Table 6**.** Two samples (S2 and S3) indicated sign of adulteration with detergents and neutralizers, while sample (S8) shows the presence of all these adulterants which were intentionally added to the sample. The results for sample S8 is shown in Figure 12. Others samples indicated no sign of adulteration with these adulterants (urea, detergents and neutralizers).

Table. 6 Analysis of different milk samples for various adulterants (detergent, urea and neutralizers), '+' indicates the presence while '-' shows the absence of particular adulterant in different samples.

Samples	Detergent	Urea	Neutralizers (Carbonates/Bicarbonates)
S1	-	-	-
S2	+	-	-
S3	-	-	+
S4	-	-	-
S5	-	-	-
S6	-	-	-
S7	-	-	-
S8	+	+	+
S9	-	-	-
S10	-	-	-
S11	-	-	-
S12	-	-	-

3.3.2 Discussion on milk adulteration

The present study is conducted to design and demonstrate a reliable paper-based microfluidic method for analysis of milk adulteration. Quality of milk is reduced by the addition of adulterants making it potentially unhealthy for consumption. This is particularly important for neonates and especially in the first few years of children when their immune system is still vulnerable. Hence, quality control tests for milk are very important to qualify the adulteration in milk and to ensure its safe consumption [27]. Milk adulteration is prohibited because of its adverse effects [30]. A chemical fertilizer, urea, is commonly used milk adulterant. It is added to the diluted milk in order to make up the lactometer reading (density) [27]. It is often used for whitening of milk [31], causing damage to heart, kidneys and liver [32]. As it is the significant component of synthetic milk, therefore, it is added to milk for promoting its SNF (solid-not-fat) value. It is also used to increase the shelf-life of milk [32]. There are many methods for the detection of adulterated milk with added urea. Naturally, urea is also present in milk. Cow milk contains about 50 mg/100 ml of natural urea on average, however, 35 mg/100 ml (average) of urea is present in buffalo milk [27]. The detection limit for detecting added urea is 0.2% [33].

Common neutralizers like carbonates (Na_2CO_3) and bicarbonates ($NaHCO_3$) are used to adulterate milk for neutralizing the appeared acidity in the milk [34]. These cause diarrhea, colon ulcers and gastric ulcers [35]. The detection limit for carbonates is 0.1% and 0.2% for bicarbonates is [34]. Some neutralizers are also components of detergents [27].

Pure milk has an excessive nutritional value. It contains significant amount of essential nutrients like proteins, carbohydrates, fats, vitamins and minerals [36]. Tragically, milk consumed by most of the people of Pakistan contains adulterants [37]. Milk dealers adulterate milk by diluting it with water and adding cheap substances in order to sustain its compositional parameters. Common adulterants include unhygienic water, starch, urea, detergents and carbonates etc., [38]. " Water, often added to dilute the milks, is obtained from unhealthy sources that may include some or all of above mentioned adulterants [39].

Among various samples tested for adulteration three samples (S2, S3 and S8) were positive (+) for adulterants. S2 was positive (+) for detergent and S3 contained neutralizers. All other samples indicated no sign of adulteration with urea, detergents and neutralizers. S8 revealed the presence of all the adulterants (intentionally added).

These devices are although reliable but can only provide qualitative analysis i.e. 'Yes/No' type of results. Because of the different ambient light condition and the wet or dry condition of paper, the colorimetric result may be interpreted different by different individuals as the colour and intensity interpretation by eye is different for each person. More investigation will be done in future to study the chemical reaction as well as modification in the shape of device to perform longer experiments without contaminating the samples.

4 Conclusions

In this research a regression model for accurate prediction of final dimensions of lines/hydrophobic: hydrophilic channels has been developed for paper based microfluidic devices. Experimental results show that this model is in agreement with empirical observations within an accuracy of 92 %. . Determination of line width and hence exact channel size of the final paper microfluidics devices can also help predict exact amount of reagents needed for microfluidic application. This can prevent waste of expensive reagents. This model will be very helpful in future, for mass-producing paper-based analytical wherein we can pre-calculate the desired dimension of the channels and barriers suited best to our desired applications. Finally, our results for milk adulteration tests on μPAD depict that colorimetric reactions can easily be done on μPADs and several independent reactions can be done simultaneously in various test zones on a device without cross-contamination of the reagents. Visualization of distinct colors on device depends on the presence or absence of adulterants.

Conflict of Interests

The authors declare that there is no conflict of interests regarding the publication of this paper.

Acknowledgments

We thank our lab colleagues Nauman Khan and Zia-ur-rehman for their handful suggestions during the lab work.

References:

1. Liana, D.D., et al., *Recent Advances in Paper-Based Sensors.* Sensors, 2012. **12**(9): p. 11505-11526.
2. Mao, X. and T.J. Huang, *Microfluidic diagnostics for the developing world.* Lab Chip, 2012. **12**(8): p. 1412-6.
3. Martinez, A.W., et al., *Patterned paper as a platform for inexpensive, low-volume, portable bioassays.* Angew Chem Int Ed Engl, 2007. **46**(8): p. 1318-20.
4. Lisowski, P. and P.K. Zarzycki, *Microfluidic paper-based analytical devices (μPADs) and micro total analysis systems (μTAS): development, applications and future trends.* Chromatographia, 2013. **76**(19-20): p. 1201-1214.
5. He, Y., et al., *Fabrication of paper-based microfluidic analysis devices: a review.* Rsc Advances, 2015. **5**(95): p. 78109-78127.
6. Nawaz, A.A., et al., *Sub-micrometer-precision, three-dimensional (3D) hydrodynamic focusing via "microfluidic drifting".* Lab Chip, 2014. **14**(2): p. 415-23.
7. Nawaz, A.A., et al., *Acoustofluidic Fluorescence Activated Cell Sorter.* Anal Chem, 2015. **87**(24): p. 12051-8.
8. Carrilho, E., A.W. Martinez, and G.M. Whitesides, *Understanding wax printing: a simple micropatterning process for paper-based microfluidics.* Anal Chem, 2009. **81**(16): p. 7091-5.
9. Lu, Y., et al., *Rapid prototyping of paper-based microfluidics with wax for low-cost, portable bioassay.* Electrophoresis, 2009. **30**(9): p. 1497-1500.
10. Dungchai, W., O. Chailapakul, and C.S. Henry, *A low-cost, simple, and rapid fabrication method for paper-based microfluidics using wax screen-printing.* Analyst, 2011. **136**(1): p. 77-82.
11. Liu, M., C. Zhang, and F. Liu, *Understanding wax screen-printing: a novel patterning process for microfluidic cloth-based analytical devices.* Anal Chim Acta, 2015. **891**: p. 234-46.
12. Fenton, E.M., et al., *Multiplex lateral-flow test strips fabricated by two-dimensional shaping.* ACS Appl Mater Interfaces, 2009. **1**(1): p. 124-9.
13. Abe, K., K. Suzuki, and D. Citterio, *Inkjet-printed microfluidic multianalyte chemical sensing paper.* Anal Chem, 2008. **80**(18): p. 6928-34.
14. Abe, K., et al., *Inkjet-printed paperfluidic immuno-chemical sensing device.* Anal Bioanal Chem, 2010. **398**(2): p. 885-93.
15. Li, X., J.F. Tian, and W. Shen, *Progress in patterned paper sizing for fabrication of paper-based microfluidic sensors.* Cellulose, 2010. **17**(3): p. 649-659.
16. Songjaroen, T., et al., *Novel, simple and low-cost alternative method for fabrication of paper-based microfluidics by wax dipping.* Talanta, 2011. **85**(5): p. 2587-93.
17. Bruzewicz, D.A., M. Reches, and G.M. Whitesides, *Low-cost printing of poly(dimethylsiloxane) barriers to define microchannels in paper.* Analytical Chemistry, 2008. **80**(9): p. 3387-3392.
18. Martinez, A.W., et al., *Simple telemedicine for developing regions: Camera phones and paper-based microfluidic devices for real-time, off-site diagnosis.* Analytical Chemistry, 2008. **80**(10): p. 3699-3707.
19. Li, X., et al., *Paper-Based Microfluidic Devices by Plasma Treatment.* Analytical Chemistry, 2008. **80**(23): p. 9131-9134.
20. Yan, C.F., et al., *Fabrication of Paper-based Microfluidic Devices by Plasma Treatment and Its Application in Glucose Determination.* Acta Chimica Sinica, 2014. **72**(10): p. 1099-1104.
21. Martinez, A.W., et al., *Diagnostics for the Developing World: Microfluidic Paper-Based Analytical Devices.* Analytical Chemistry, 2010. **82**(1): p. 3-10.
22. Renault, C., et al., *Three-Dimensional Wax Patterning of Paper Fluidic Devices.* Langmuir, 2014. **30**(23): p. 7030-7036.

23. Zhong, Z.W., Z.P. Wang, and G.X.D. Huang, *Investigation of wax and paper materials for the fabrication of paper-based microfluidic devices.* Microsystem Technologies-Micro-and Nanosystems-Information Storage and Processing Systems, 2012. **18**(5): p. 649-659.
24. Lu, Y., B. Lin, and J. Qin, *Patterned paper as a low-cost, flexible substrate for rapid prototyping of PDMS microdevices via "liquid molding".* Anal Chem, 2011. **83**(5): p. 1830-5.
25. Pereverzeva, L.P., A.N. Pereverzev, and R.A. Martirosov, *Influence of Properties of Wax Compositions on Water-Vapor Permeability of Packaging Paper.* Chemistry and Technology of Fuels and Oils, 1984. **20**(5-6): p. 305-306.
26. Washburn., E.W., *The dynamics of capillary flow.* Physical review, 1921.
27. Kamthania, M., et al., *Milk Adultration: Methods of Detection &Remedial Measures.* Int. J. Engg. and Technical Res, 2014. **1**: p. 2321-0869.
28. Carrilho, E., A.W. Martinez, and G.M. Whitesides, *Understanding Wax Printing: A Simple Micropatterning Process for Paper-Based Microfluidics.* Analytical Chemistry, 2009. **81**(16): p. 7091-7095.
29. Li, R., et al., *Solidification contact angles of molten droplets deposited on solid surfaces.* Journal of Materials Science, 2007. **42**(23): p. 9511-9523.
30. Ayub, M., et al., *Composition and adulteration analysis of milk samples.* 2007.
31. Walker, G.P., F.R. Dunshea, and P.T. Doyle, *Effects of nutrition and management on the production and composition of milk fat and protein: a review.* Crop and Pasture Science, 2004. **55**(10): p. 1009-1028.
32. Das, S., B. Goswami, and K. Biswas, *Milk Adulteration and Detection: A Review.* Sensor Letters, 2016. **14**(1): p. 4-18.
33. Bector, B., M. Ram, and O. Singhal, *Rapid platform test for the detection/determination of added urea in milk.* Indian Dairyman, 1998. **50**: p. 59-62.
34. Upadhyay, N., et al., *Preservation of milk and milk products for analytical Purposes.* Food Reviews International, 2014. **30**(3): p. 203-224.
35. Beall, D.P. and H.R. Scofield, *Milk-Alkali Syndrome Associated with Calcium Carbonate Consumption: Report of 7 Patients with Parathyroid Hormone Levels and an Estimate of Prevalence Among Patients Hospitalized with Hypercalcemia.* Medicine, 1995. **74**(2): p. 89-96.
36. Neumann, C., D.M. Harris, and L.M. Rogers, *Contribution of animal source foods in improving diet quality and function in children in the developing world.* Nutrition Research, 2002. **22**(1): p. 193-220.
37. Loudon, I., *Deaths in childbed from the eighteenth century to 1935.* Medical History, 1986. **30**(01): p. 1-41.
38. Tipu, M.S., et al., *Monitoring of chemical adulterants and hygienic status of market milk. Handbook published by Quality Control Laboratory, Univ. Vet.* Anim. Sci., Lahore, Pakistan. pp, 2007. **7**.
39. Kasemsumran, S., W. Thanapase, and A. Kiatsoonthon, *Feasibility of near-infrared spectroscopy to detect and to quantify adulterants in cow milk.* Analytical Sciences, 2007. **23**(7): p. 907-910.

Electronic Supplementary material

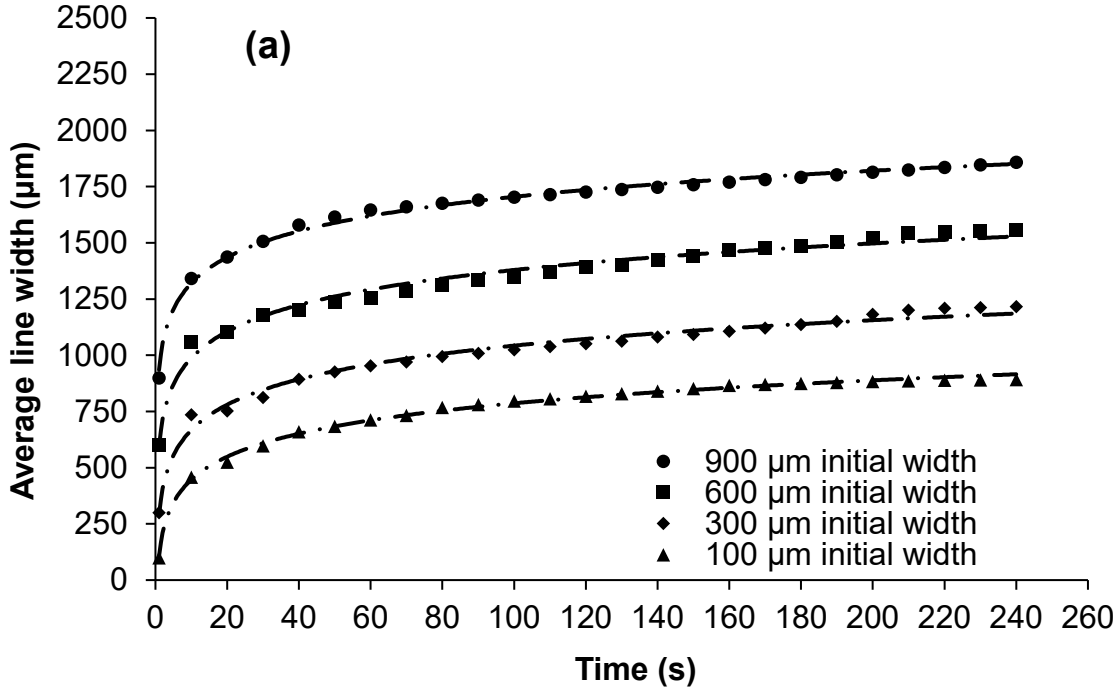

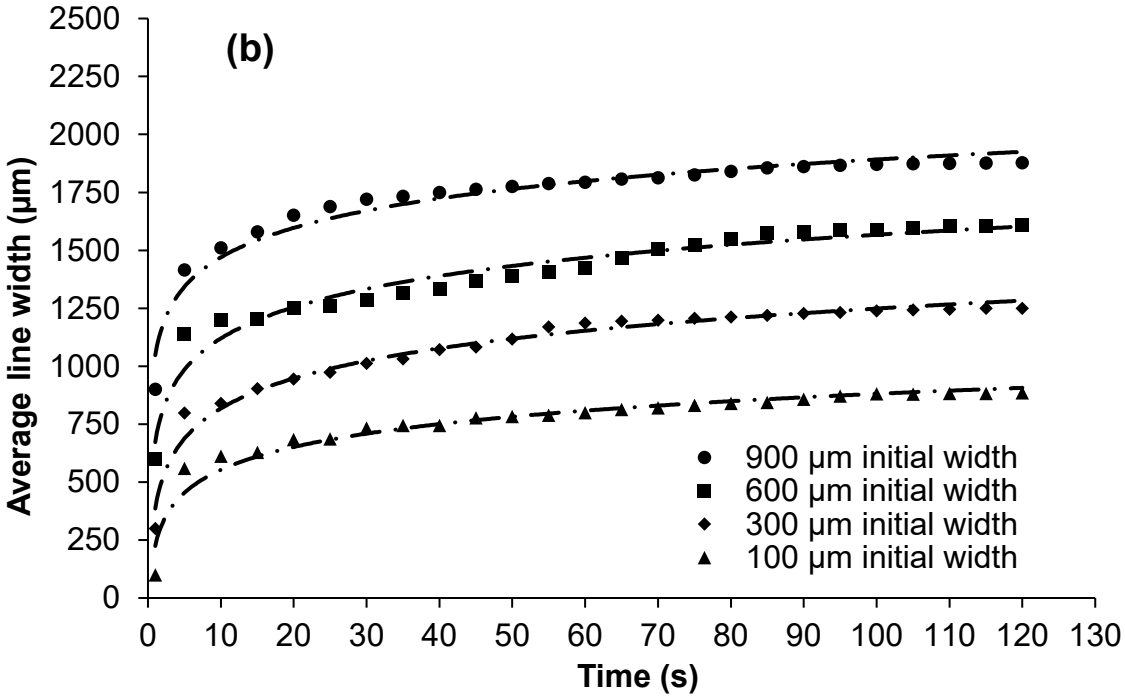
(b)
Average line width (µm)
Time (s)
900 µm initial width
600 µm initial width
300 µm initial width
100 µm initial width

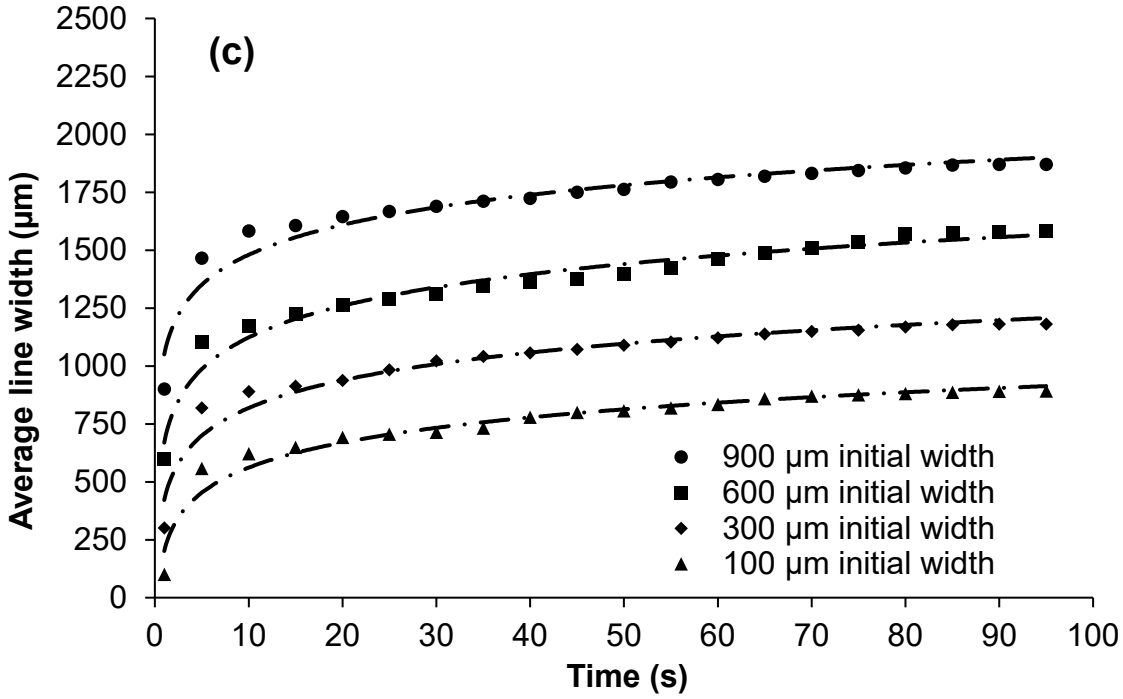
(c)
Average line width (µm)
Time (s)
900 µm initial width
600 µm initial width
300 µm initial width
100 µm initial width

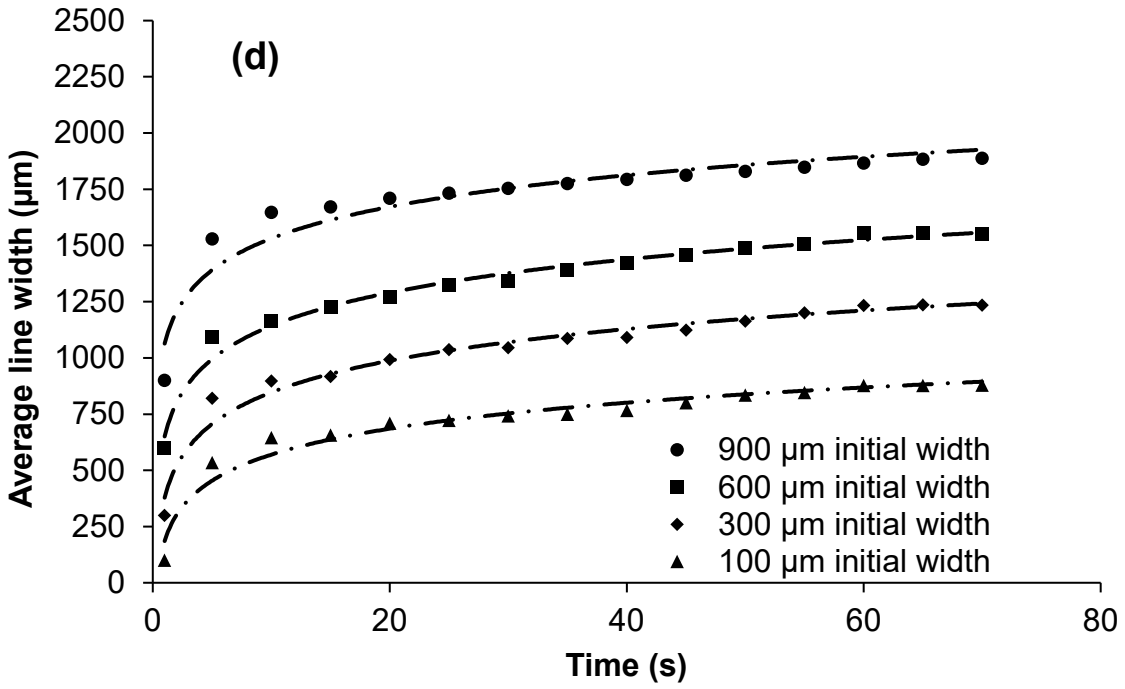

Fig. 1 The effect of different initial line thickness on final spreading at (a) temperature 90 ºC, (b) temperature 110 ºC, (c) temperature 130 ºC and (d) temperature 150 ºC

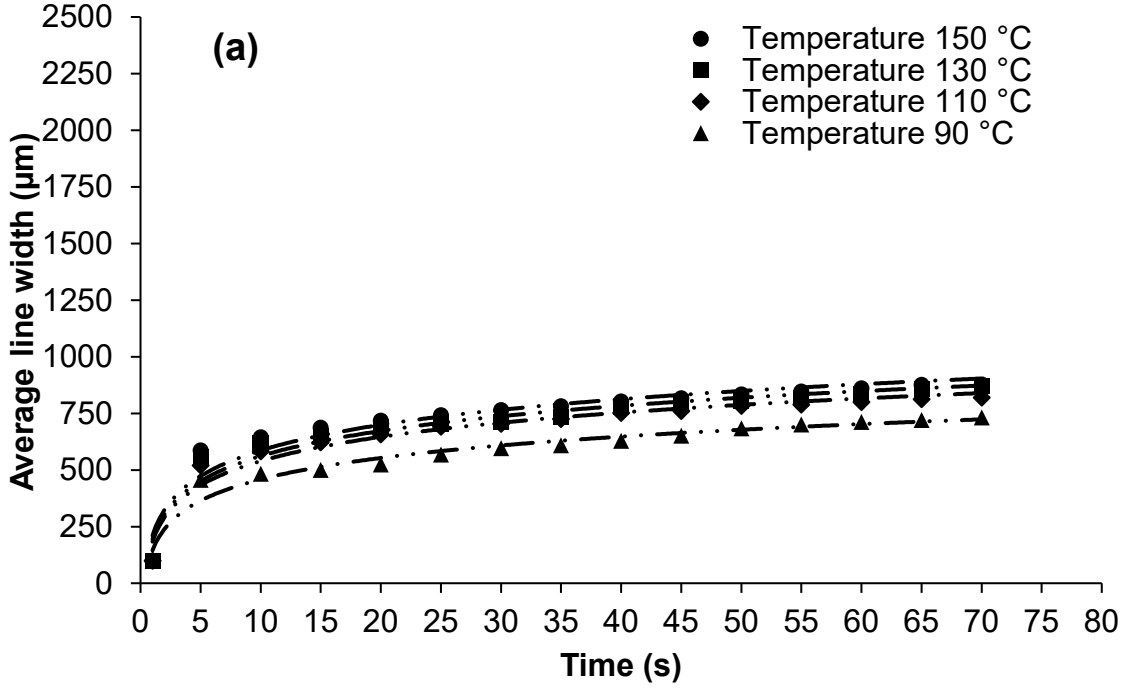

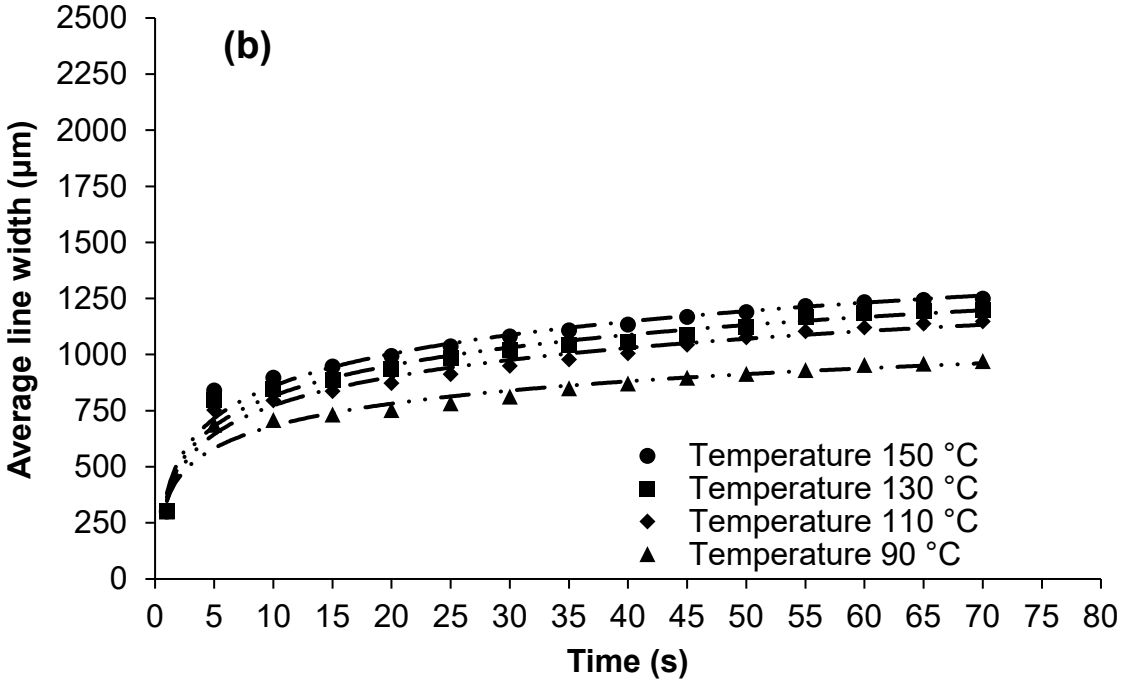
(b)
Average line width (µm)
2500
2250
2000
1750
1500
1250
1000
750
500
250
0
0 5 10 15 20 25 30 35 40 45 50 55 60 65 70 75 80
Time (s)
Temperature 150 °C
Temperature 130 °C
Temperature 110 °C
Temperature 90 °C

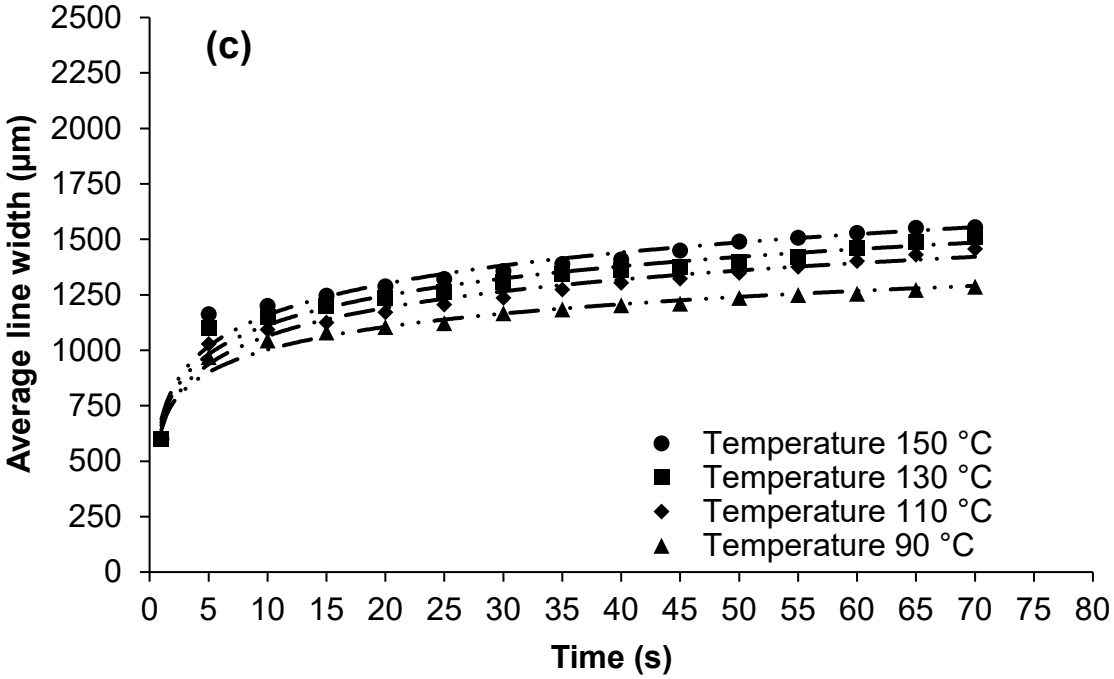
(c)
Average line width (µm)
2500
2250
2000
1750
1500
1250
1000
750
500
250
0
0 5 10 15 20 25 30 35 40 45 50 55 60 65 70 75 80
Time (s)
Temperature 150 °C
Temperature 130 °C
Temperature 110 °C
Temperature 90 °C

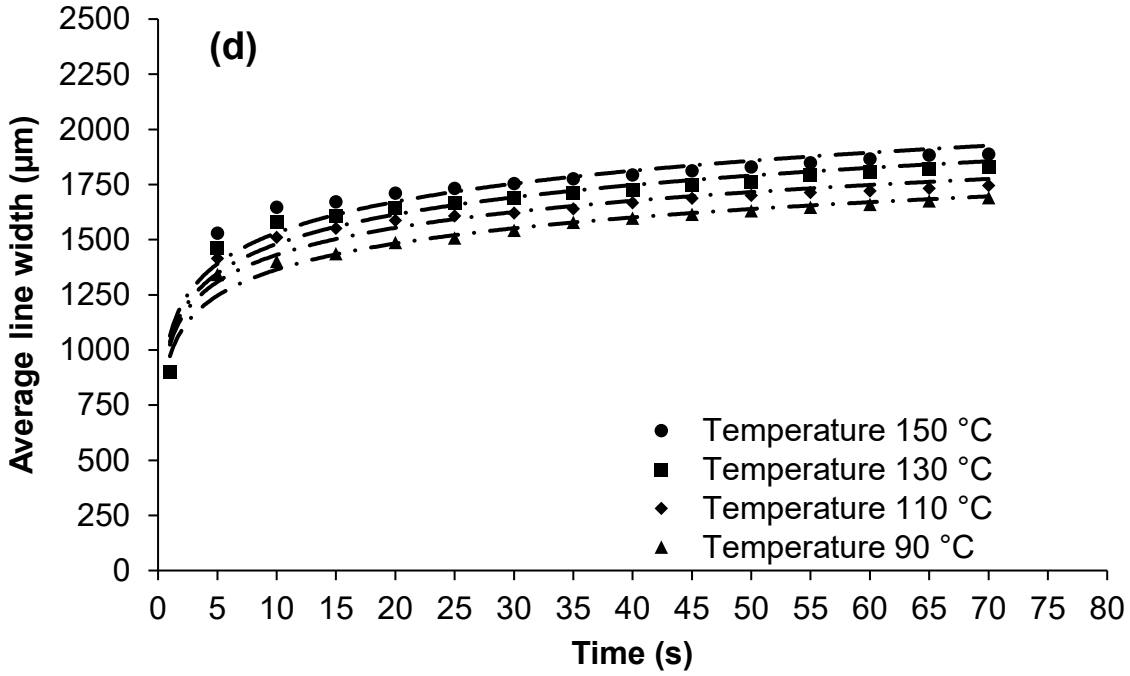

Fig. 2 Spreading of wax at different temperatures (90 ºC, 110 ºC, 130 ºC and 150 ºC) for (a) 100 µm initial thickness, (b) 300 µm initial thickness, (c) 600 µm initial thickness and (d) 900 µm initial thickness

Table. 1 Change in width of the printed line at different time intervals 5 secs, 100 secs and 240 secs (at temperature 90 ºC)

Line width	Change in width after 5 seconds	Change in width after 100 seconds	Change in width after 240 Seconds
100 µm	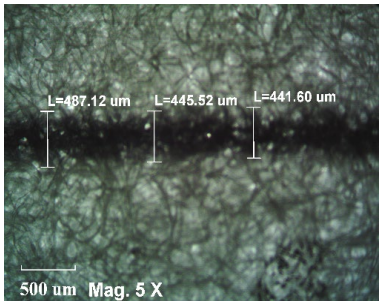	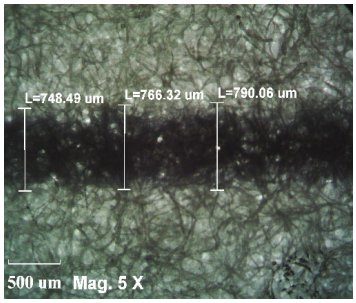	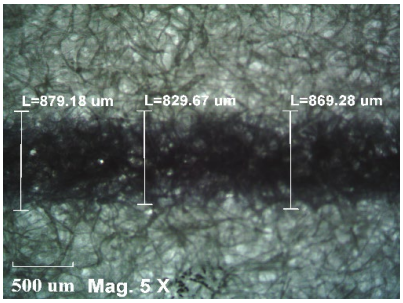
300 µm	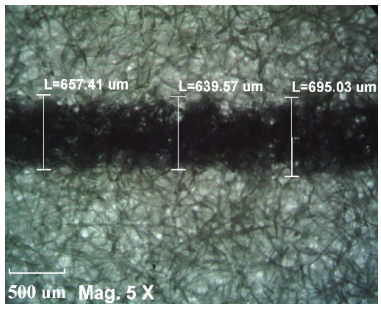	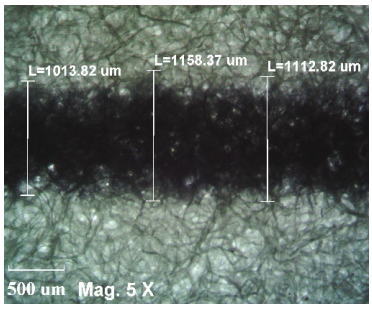	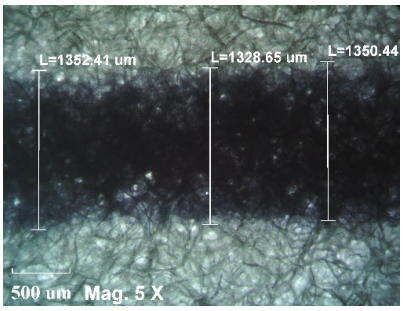
900 µm	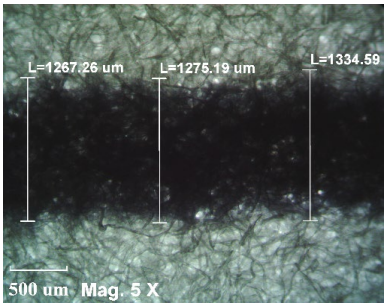	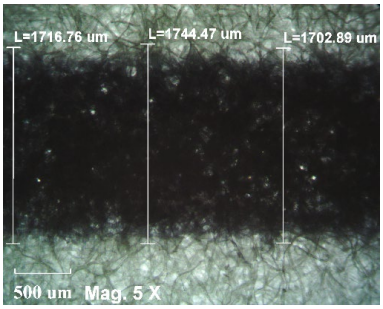	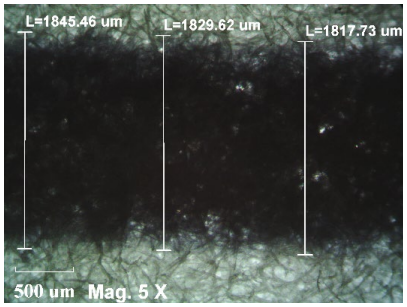

Table. 2 Change in width of the printed line at different time intervals 5 secs, 35 secs and 70 secs (at temperature 150 ºC)

Line width	Change in width after 5 secs	Change in width after 35 secs	Change in width after 70 secs
100 µm	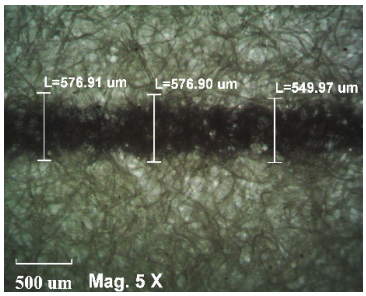	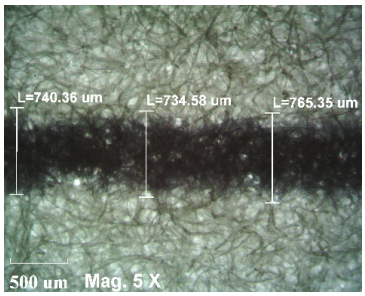	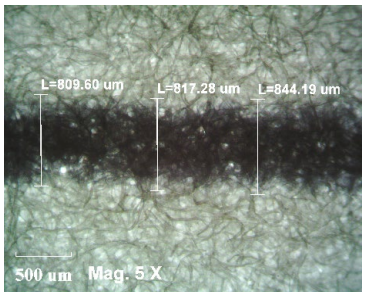
300 µm	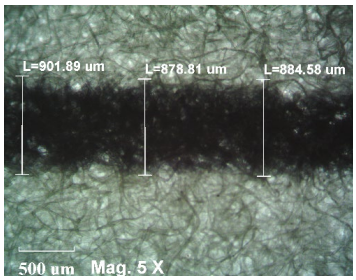	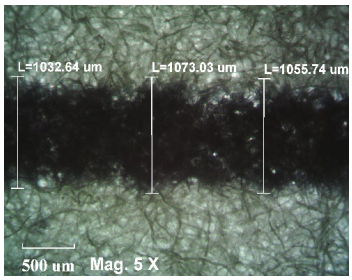	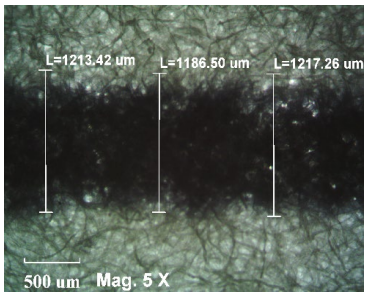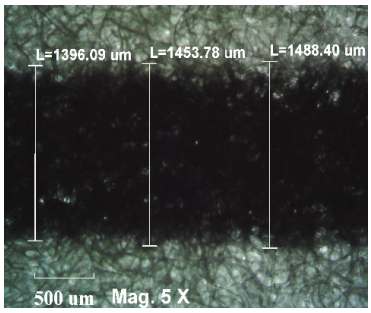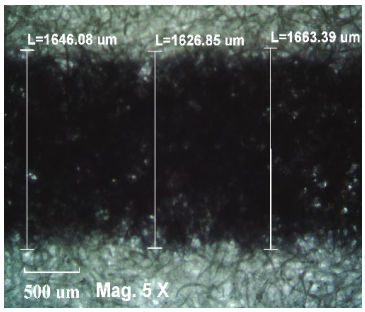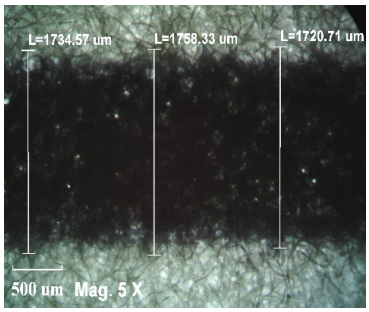
900 µm